IBIMA Publishing
Communications of International Proceedings
https://ibimapublishing.com/p-articles/47ICT/2026/4732526/
Vol. 2026 (13), Article ID 4732526

Real-Time Wireless Position and Angle Measurement System for IoT and Vehicle Telemetry*

Przemysław WOJCIESZCZAK, Daniel PRUSAK AND Grzegorz KARPIEL

RIOT sp. z o.o., ul. M. i B. Wysłouchów 26/26, 30-612 Kraków.
AGH University of Krakow, Faculty of Mechanical Engineering and Robotics, Department of Robotics and Mechatronics, Al. Mickiewicza 30, 30-059 Kraków

Correspondence should be addressed to: Przemysław WOJCIESZCZAK, pwoj@agh.edu.pl

*Presented at the 47th IBIMA International Conference, 29-30 June 2026, Madrid, Spain

Abstract

The article describes a system of wireless measurements that can be used in the IoT or vehicle telemetry. Today, IoT systems are everywhere. The sensors of these systems collect various data. Then, all data must be sent to the main unit that can use them for diagnostic purposes or for control. Data should be sent as fast as possible. It would be best if the data were sent in real time. The same situation is in the vehicle telemetry system, especially for autonomous vehicles. This task may be performed using a small reflective absolute encoder with an embedded system based on the popular ESP32 chip. The document presents the initial phase of testing of the wireless data acquisition system. The study was motivated by the desire to build a system capable of real-time data transmission that was as compact as possible and based on widely available and low-cost components. To this end, the focus was placed on a relatively new solution: the Espressif-developed ESP-NOW protocol. During the tests, several important aspects were examined from the perspective of the telemetry system. One of them was the maximum distance between the transmitter and receiver under actual operating conditions. Subsequent aspects were the power consumption depending on the configured transmitter power, time required to complete a work cycle, and the time between sending a message and receiving a reply.

Keywords: ESP32, wireless data acquisition, reflective encoder, IoT, control system

Introduction

Nowadays, data are one of the most important things in the world. Sensors are everywhere. They collect information on temperature, pressure, magnetic field, our position, and much more. This data is used for various purposes, for example, for statistics purposes, for control systems, to optimize certain processes, or for healthcare. (Anderson, 2008; Saylan and Denizli, 2020; Torkey et al., 2022).

Telemetry systems collect data from the sensors and send them further. These systems are specially built for all types of mobile units. They can be found in moving vehicles, aerial vehicles, and even rockets. This shows why a telemetry system is ubiquitous (Vasylenko and Karpyuk, 2018; Anggara Trisna Nugraha and Priyambodo, 2020).

The range of telemetry system vary and depends on the individual case. Sometimes, only data transmission over a few meters is enough, but sometimes it is necessary to transmit data over hundreds of kilometers or even

Cite this Article as: Przemysław WOJCIESZCZAK, Daniel PRUSAK AND Grzegorz KARPIEL Vol. 2026 (13) “Real-Time Wireless Position and Angle Measurement System for IoT and Vehicle Telemetry " Communications of International Proceedings, Vol. 2026 (13), Article ID 4732526, https://doi.org/10.5171/2026.4732526

thousands of kilometers. Various forms of communication may be used (Morollón et al., 2022; Niwa and Sawai, 2021).

In the case of vehicles, for example cars, there are many different sensors. They are used for control, but also for diagnostic purpose. Components such as encoders are used in the steering system. They can also be used in the suspension or in the throttle of the car. In mobile robots, encoders are widely used. They can be used in adaptive suspension. It will adapt to the ground so that all wheels have contact with the ground. Encoders can also be used in the drive system. Thanks to them, it is possible to implement appropriate control loops for motors.

Nowadays, autonomous vehicles are becoming more and more common. Not only cars but also mobile robots. Very often there is no human in their work environment. In the event of failure, without the telemetry system it will be impossible to notice that fact and repair them as quickly as possible. Therefore, the time from failure to repair is shorter when a telemetry system is used. We also got more information on the causes and circumstances in which this situation occurred. Therefore, we can make improvements and minimize the risk of repeat failure. In addition, we can use the telemetry system for diagnostic purposes. We can use a temperature sensor or vibration sensor to detect signs of future damage. For example, we can measure the temperature and vibration of bearings. This parameter will allow us to estimate when the bearing will be damaged and replace it earlier, planning this operation, and reserving the necessary funds. Due to this, the repair time will be shorter and the costs will decrease (SKF, 2025; Bhonde and Panchwadkar, 2023).

In IoT encoders are widely used. In smart home applications they are used to control roller shutters or gates and window drives. They are also used in the home weather station. Thanks to them, it is possible to determine the wind speed and direction. In industry 4.0 encoders are used to monitor rotational speed of some machines or angular/linear position. In that case, one person can supervise the operation of many machines. Encoders are also widely used in the renewable energy industry. With them, it is possible to place the wind turbine blades in the optimal position. Encoders are also used in solar-tracking photovoltaic panel farms.

Construction of wireless data acquisition system

This article presented the system of acquisition of data from absolute position, wireless sensor. The sensor measures a linear or angular position depending on the target used. There are many decoder disks and encoder rulers of different sizes with which the encoder can work. For research purposes, some versions of the dedicated PCB were designed and assembled. All of them contain a small encoder chip and power supplies for it. Some of them also contain an ESP32 chip. The sensor block diagram presented in Figure 1 shows all parts of the system.

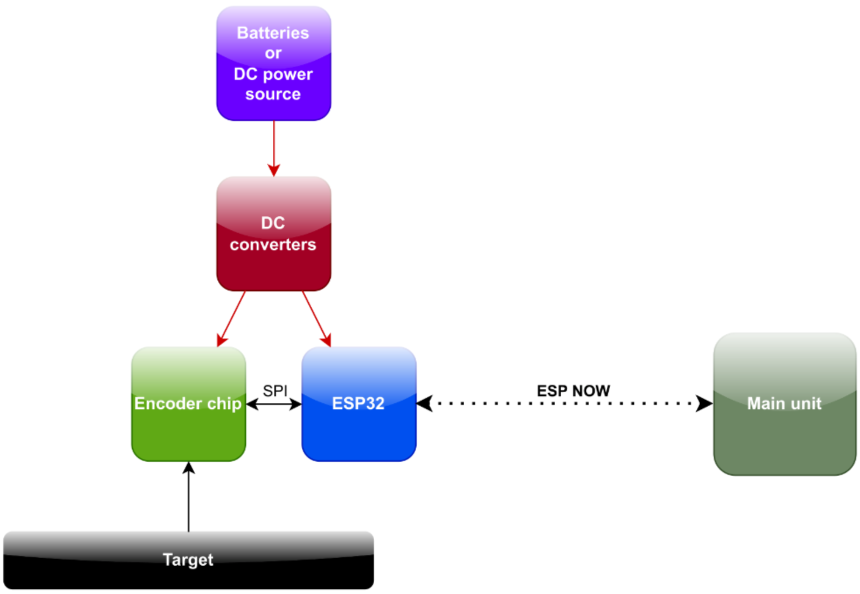

Figure 1. Block diagram of the sensor.

The sensor consisted of the following subsystems:

- **Batteries or DC power source**
  In the first version, the sensor could be powered with a voltage in the range of 6-60V DC or 5V DC. In subsequent versions, the power supply system was redesigned. It allows sensor to be supplied from CR2032 batteries at a voltage of 3V DC.

- **DC converters**
  In the first version of sensor the DC-DC Step-Down converter was designed. In the next versions, DC-DC Step-Up converters were used.

- **Encoder chip**
  The encoder chip was the reflective encoder.

- **ESP32**
  For data acquisition, the ESP32C3 chip was used. It had enough computing power, to get data about a position from the encoder chip. It also consumed little energy. So, it was a perfect solution for the later version of the PCBs, which were powered from batteries.

- **Main unit**
  ESP32S3 was chosen as the main device. It had enough computing power to receive data from multiple sensors and then process it.

- **Target**
  The target was the encoder disk or the encoder linear scale.

Choosing the data acquisition interface

The encoder chip has multiple communication interfaces. Among other things, it has:

- Serial Peripheral Interface (SPI),
- Synchronous Serial Interface (SSI),
- Bidirectional Serial Synchronous Interface (BiSS Interface),
- Absolute Data Interface (ADI).

In addition to these interfaces, it is also possible to read the encoder data in another form. For example, it is possible to use:

- ABZ generator,
- UVW generator,
- analog.

During the research process, multiple methods of data acquisition were tested. The appearance of the test stand is shown in Figure 2.

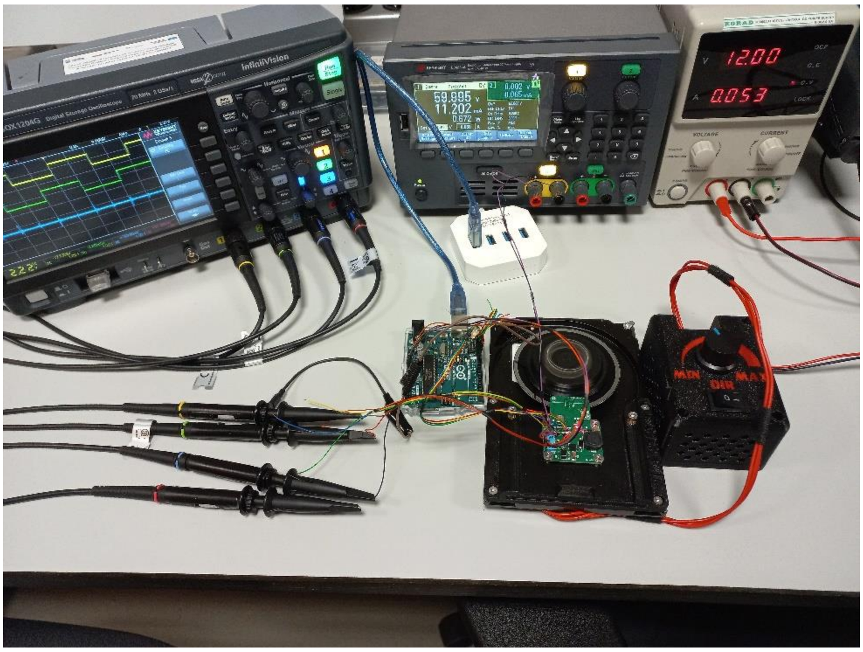

Figure 2. Test stand.

The test stand contains the following:

- PC,
- laboratory power supply (KEYSIGHT E36234A),
- laboratory power supply (KORAD KD3005D),
- Arduino UNO R3,
- BLDC motor,
- BLDC motor controller,
- oscilloscope (KEYSIGHT DSOX1240G),
- target - encoder disk,
- first version of PCB.

The first version of the sensor's PCB is presented in Figure 3.

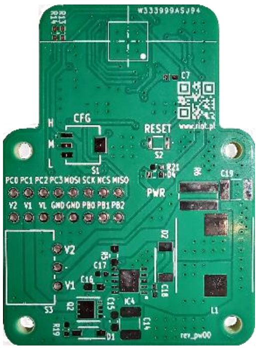

Figure 3. First version of sensor's PCB.

The first version of the sensor allows for testing multiple interfaces.

Figure ***4*** shows the test results.

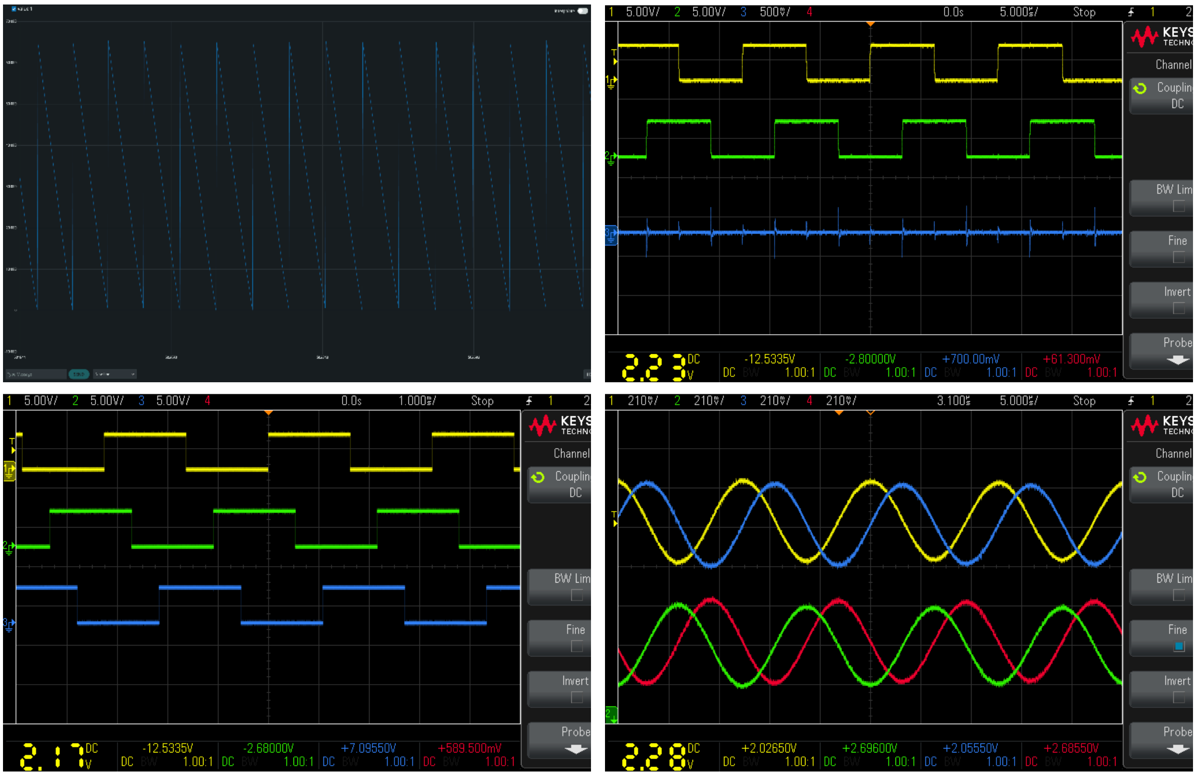

Figure 4. Test results.

The absolute position red through the SPI interface is shown in the upper left corner of the

Figure *4*. The vertical axis of the graph represented the absolute position measured by the encoder and the horizontal axis of the graph represented the sample number. The SPI interface was tested because it is easy to implement on most development boards like Arduino, ESP32, STM or Microchip.

The oscillogram of the ABZ generator is shown in the upper right corner. The yellow signal came from channel A of the encoder, the green signal came from channel B, and the blue signal was a signal Z. The results achieved during the UVW generator are shown in the lower left corner. The results of the analog output are presented in the lower right corner. The signals presented were positive and negative sine signal and positive and negative cosine signal.

Data acquisition from encoder

Data transfer between sensor and main unit

In the project sensor and main unit based on ESP32 chips. Therefore, for communication purposes, the ESP-NOW protocol was used. This solution does not need any WiFi router. ESP-NOW based on the MAC addresses of the devices. The range of this protocol is from several dozen to even several hundred meters. Moreover, this solution is very fast and consumes a little energy. During tests, the sensor worked according to the diagram shown in Figure 8.

As shown in Figure 8 the data transfer was based on sending two messages. The first one was sent from the sensor to the main unit and contains information about absolute position. The second was sent from the main unit to the sensor and was just a confirmation of data receipt. After receiving that confirmation, ESP32 went into Deep-sleep mode. In this mode, CPU, RF circuits and most other components are disabled. Only RTC timer and RTC memory are enabled. According to technical documentation, during this mode, the current consumption is about 5 µA. This allows the sensor to operate for a long time, even on battery power. There are several ways to exit Deep-sleep mode. During tests. The RTC timer was used to wake up ESP32 (Esspressif, 2026).

In the ESP-NOW protocol it is necessary to prepare a data frame for sending. It should look the same for the transceiver and for the receiver. For research purposes, the data frame contains:

- Sensor ID

This number was used to identify which sensor transmitted the position data.

- Sensor status

This number was used for diagnosis purposes. For example, it informed whether the sensor was configured.

- Current time

This data was used to synchronize the time of the sensor and the main device.

- Target time

This data was used to determine the time of the next measurement.

- Current position

This data was used to inform the main device about the current position.

- MAC address of the main unit

This data was used for sensor configuration purposes. This allowed new sensors to be dynamically added to the main unit.

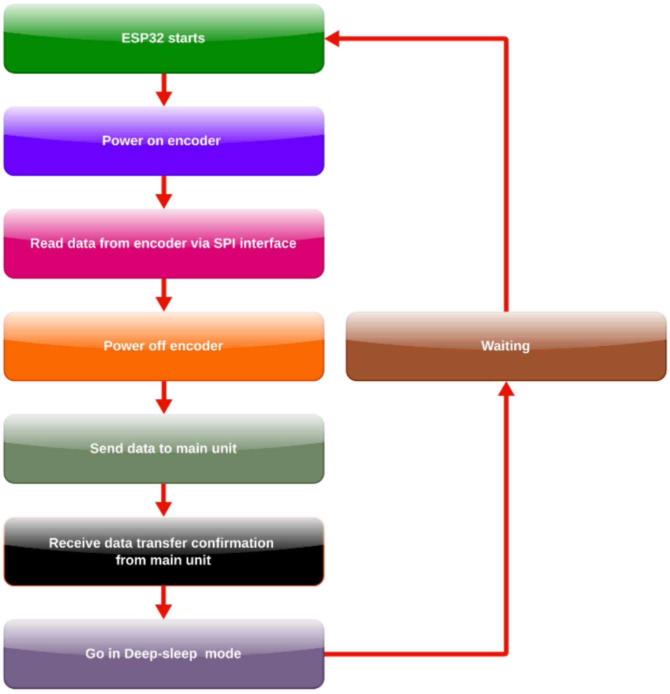

Figure 8. Block diagram od sensor operation.

The maximum length of the frame is different depending on the version of the ESP-NOW protocol. For version 1.0 maximum packet length is 250 bytes, but for version 2.0 this length increases to 1470 bytes.

Main unit and sensor synchronization

Time synchronization between the main unit and the sensors was important. The main unit was continuously powered. Therefore, it could synchronize it's time with SNTP server. However, sensors need to save energy. In that case, they cannot just connect to the SNTP server and synchronize their time. Therefore, information on the current time was sent to them with a transmission confirmation frame. However, this did not completely solve the time synchronization problem. There was still a problem with time drift on RTC timer during Deep-sleep mode. This problem was solved by changing the default internal slow RTC timer to the faster one. According to the technical documentation, this resulted in an increase in current consumption of 5 μA. However, this current consumption level was still acceptable.

Data transmission speed test

For research purposes, different cases of transmission speed tests have been carried out. In the first case, how much time passes between sending the data frame by the sensor and receiving data reception. Measurements were carried out by reading the ESP32 system time value when sending data and then when receiving confirmation. The difference in these measurements was the desired result. Forty measurements were made. Their results are presented in the Figure 9.

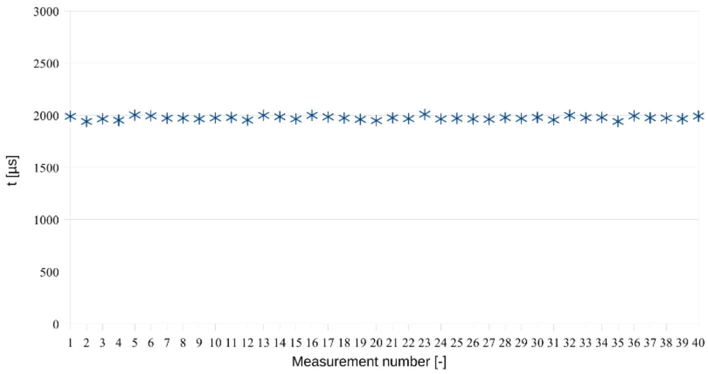

Figure 9. Time measured between data sending and receiving data reception.

The average time for this process was 1974 μs. In the second case, it was checked, how much time passes between during one full cycle of sensor work. These results are presented in Figure 10.

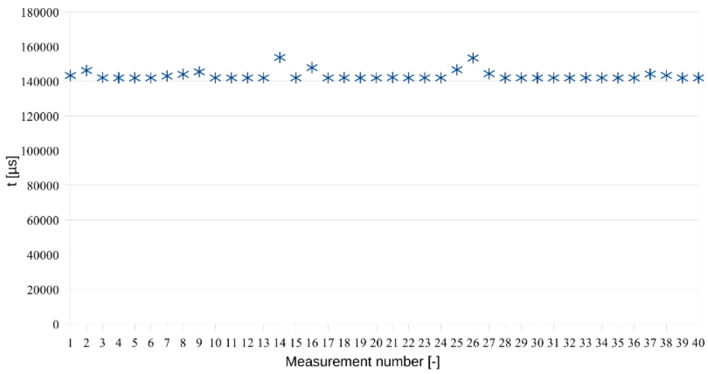

Figure 10. Time measured for one work cycle of sensor.

The average time for one sensor cycle was 143233 μs. In the third case, it was checked, how long the encoder is powered on during one sensor work cycle was measured. The results are presented in Figure 11.

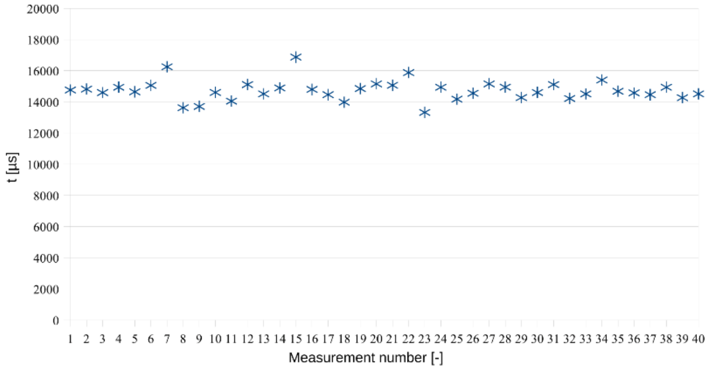

Figure 11. Time for which encoder was turned on.

The average measured time was 14729 µs. In the last case, it was checked, how long the WiFi module is powered on during one sensor work cycle was tested. The results are presented in Figure 12.

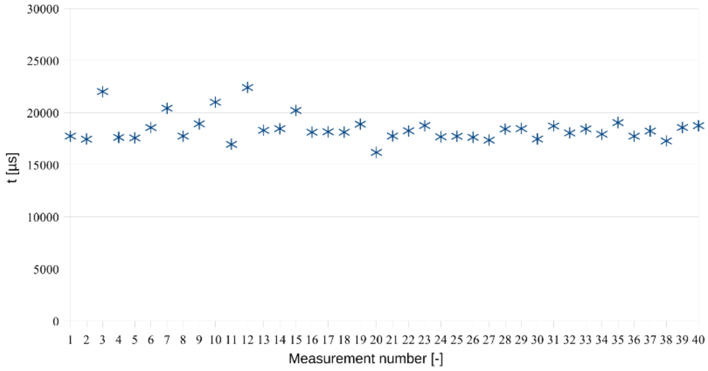

Figure 12. Time for which the WiFi module was turned on.

The average measured time was 18438 µs.

Current consumption during the work cycle of sensor.

During the research, the power consumption of the senor was measured. One measurement lasted 30 seconds, and during it, the sensor performed 8 work cycles. During tests a digital multimeter was used (KEYSIGHT 34465A). Data samples were taken every millisecond. The results are presented in Figure 13.

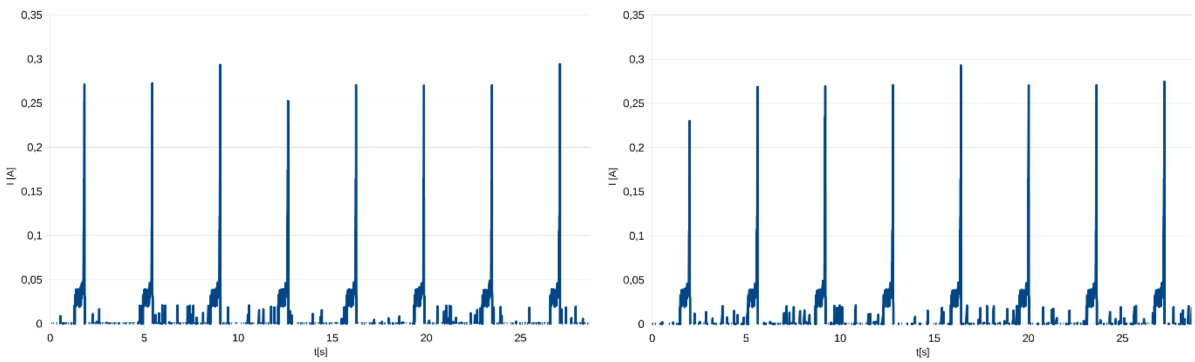

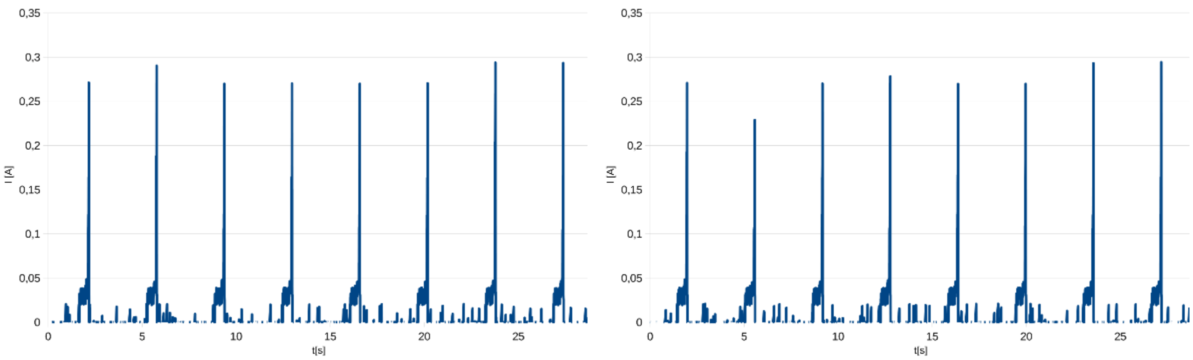

Figure 13. Measurements of current consumption.

Then the digital multimeter was switched to Digitzer Mode. The sampling frequency was set to 50kHz. With these settings, it was possible to record a signal duration of only one second. Consequently, the frequency of sending subsequent data frames has been increased. The purpose of this was to record a greater number of changes in power consumption caused by the activation of the transmitter. The transmitter power was varied. Five measurements were taken for each setting. The maximum current consumption was determined from each measurement. Subsequently, the average current consumption was calculated for each power level. Receiver was turned on. Tab. 1 presents the obtained results.

Tab. 1. Average current consumption when receiver was turned on.

Power [dBm]	Maximum current [mA]					Average maximum current [mA]
2	227,28	227,67	227,97	227,35	228,12	227,68
4	232,37	231,25	232,50	232,57	232,57	232,25
6	235,37	235,86	235,89	236,06	235,40	235,72
8	238,38	239,29	238,77	240,23	239,78	239,29
10	250,93	250,57	252,36	251,43	252,16	251,49
12	267,30	270,15	269,24	269,26	269,74	269,14
14	290,05	292,98	296,05	294,78	294,76	293,72
16	326,29	326,91	332,37	331,03	329,50	329,22
18	379,39	375,14	373,09	372,25	371,86	374,35
20	408,74	429,40	430,04	432,52	433,29	426,80

Moreover, the results are also summarized in **Figure *14***.

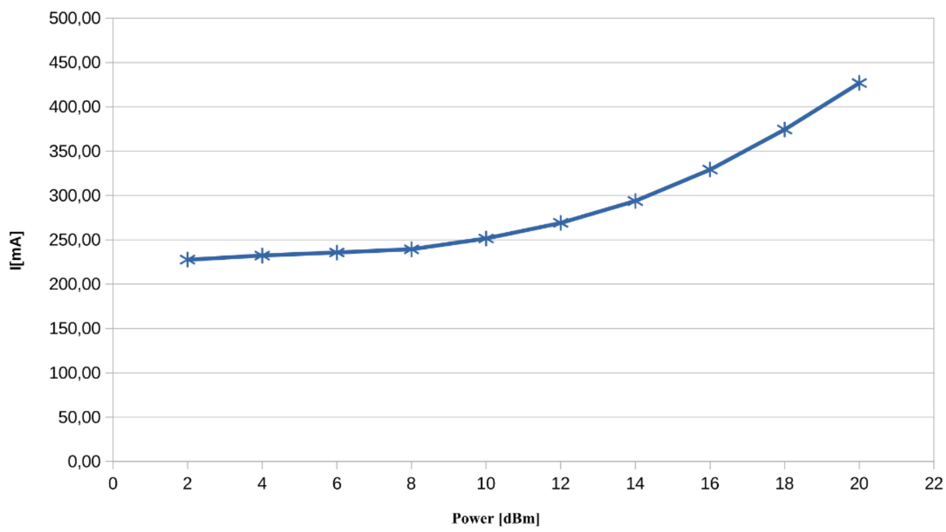

Figure 14. Average power consumption when receiver was turned on.

The same procedure was repeated for the second case – when receiver was turned off. Results from this test are presented in **Tab.** *2* and in **Figure** *15*.

Tab. 2. Average current consumption when receiver was turned off.

Power [dBm]	Maximum current [mA]					Average maximum current [mA]
2	222,80	223,94	223,67	222,22	222,97	223,12
4	225,57	224,58	228,47	227,41	230,55	227,32
6	230,68	230,81	232,74	231,45	232,26	231,59
8	236,50	230,80	236,81	237,74	235,14	235,40
10	245,90	244,48	241,11	246,60	249,56	245,53
12	260,03	257,91	259,25	256,95	256,80	258,19
14	282,44	278,60	278,93	280,90	279,29	280,03
16	318,36	314,14	312,31	314,89	309,11	313,76
18	360,23	357,08	360,13	351,66	358,89	357,60
20	443,11	428,99	409,67	412,25	408,74	420,55

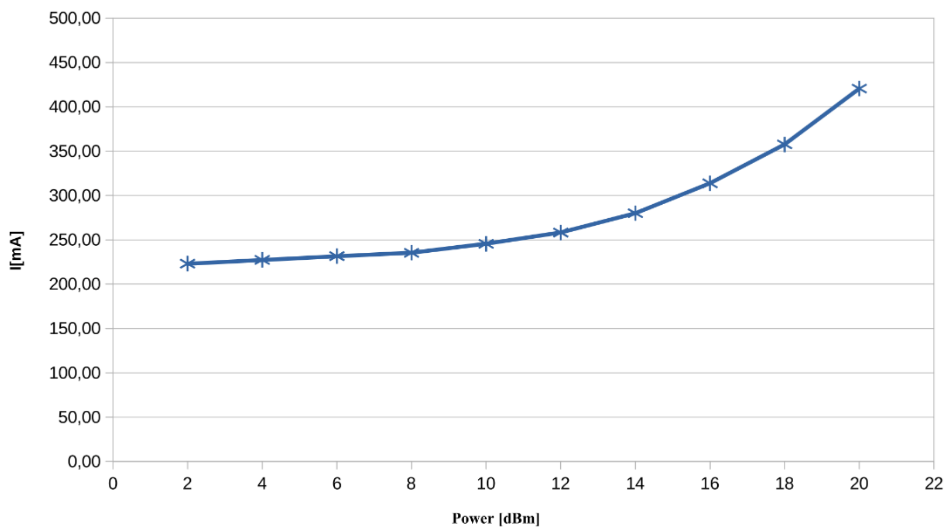

Figure 15. Average power consumption when receiver was turned off.

To facilitate data comparison, data from the two experiments have been plotted on a single graph - **Figure *16*.**

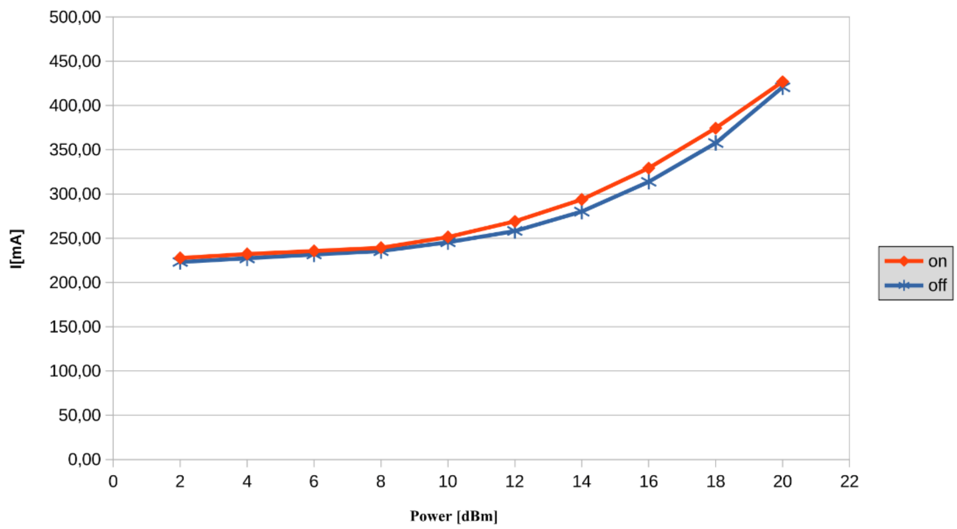

Figure 16. Comparison of results.

The resulting graphs looked similar, differing only in the levels of the values.

Frame encryption

Today, the security of transmitted data is one of the most important factors in telemetry systems. Consequently, encryption of transmitted data was ensured during the project's development. There are three options for securing data in ESP-NOW:

- **Cleartext transmission** - in this option transmitted data frames are not encrypted. It is very easy to identify data frames as frames transmitted via ESP-NOW. Moreover, it is easy to sniff the data included in frames.
- **ECDH-based** - in this option frame transmission is partially encrypted. The Vendor Specific Content header is still easily to read out, but body of the frame is encrypted. It is not necessary to share cryptographic keys. They are exchanged at the beginning of the session. An outsider can see that it is being transmitted via ESP-NOW but is unable to view the data itself.

- **Full-encryption** - in this option both the Vendor Specific header and frame body are encrypted using CCMP method. The PMK(Primary Master Key) and LMK(Local Master Key) need to be generated, each 16 byte length. PMK is used for encryption purposes of LMK. The AES-128 algorithm is used. Then LMK of the paired device is used to encrypt the data frame using the CCMP method. An outsider cannot see that the frame is being transmitted via ESP-NOW. Moreover, he cannot view the data itself.

During research the last method of data encryption was used. Data transmission security was the most important factor in choosing this method. (Espressif, 2025; Nozomi Network 2025).

Distance test and radio power

The research also focused on the aspect of the range of data transmission in relation to the transmitter power. The tests were conducted in an underground garage. The sensor was sending frames to the server and waiting for a response. For each distance, a test was conducted at various transmitter power levels. In addition, the tests were performed three times for each power level. During each experiment, 1000 frames of data were sent. The result of the test was the number of frames received by the sensor. These data are presented in **Tab.** ***3***.

Tab. 3. Results.

	Distance [m]												
Power [dBm]	**0.5**	**1**	**2**	**5**	**10**	**20**	**30**	**40**	**50**	**60**	**70**	**80**	**90**
2	1000	1000	1000	1000	1000	1000	1000	501	0	999	0	0	0
	1000	1000	1000	1000	1000	1000	1000	839	0	716	0	0	0
	1000	1000	1000	1000	1000	1000	1000	590	0	1000	0	0	0
4	1000	1000	1000	1000	1000	1000	1000	582	0	1000	4	139	0
	1000	1000	1000	1000	1000	1000	1000	980	0	1000	0	136	0
	1000	1000	1000	1000	1000	1000	1000	200	0	1000	0	289	0
6	1000	1000	1000	1000	1000	1000	1000	725	72	1000	626	988	0
	1000	1000	1000	1000	1000	1000	1000	487	502	1000	103	1000	0
	1000	1000	1000	1000	1000	1000	1000	317	954	1000	556	1000	0
8	1000	1000	1000	1000	1000	1000	1000	1000	781	1000	906	1000	29
	1000	1000	1000	1000	1000	1000	1000	1000	206	1000	886	1000	0
	1000	1000	1000	1000	1000	1000	1000	1000	575	1000	682	1000	0
10	1000	1000	1000	1000	1000	1000	1000	1000	352	1000	734	1000	2
	1000	1000	1000	1000	1000	1000	1000	1000	966	1000	999	1000	115
	1000	1000	1000	1000	1000	1000	1000	1000	198	1000	998	1000	0
12	1000	1000	1000	1000	1000	1000	1000	1000	829	1000	999	1000	963
	1000	1000	1000	1000	1000	1000	1000	1000	920	1000	1000	1000	956
	1000	1000	1000	1000	1000	1000	1000	1000	944	1000	1000	1000	685
14	1000	1000	1000	1000	1000	1000	1000	1000	1000	1000	1000	1000	989
	1000	1000	1000	1000	1000	1000	1000	1000	1000	1000	1000	1000	999
	1000	1000	1000	1000	1000	1000	1000	1000	1000	1000	1000	1000	987
16	1000	1000	1000	1000	1000	1000	1000	1000	967	1000	1000	1000	991
	1000	1000	1000	1000	1000	1000	1000	1000	944	1000	1000	1000	1000
	1000	1000	1000	1000	1000	1000	1000	1000	999	1000	1000	1000	1000
18	1000	1000	1000	1000	1000	1000	1000	1000	1000	1000	1000	1000	1000
	1000	1000	1000	1000	1000	1000	1000	1000	997	1000	1000	1000	1000
	1000	1000	1000	1000	1000	1000	1000	1000	1000	1000	1000	1000	1000
20	1000	1000	1000	1000	1000	1000	1000	1000	1000	1000	1000	1000	1000
	1000	1000	1000	1000	1000	1000	1000	1000	1000	1000	1000	1000	1000
	1000	1000	1000	1000	1000	1000	1000	1000	1000	1000	1000	1000	1000

Then, the average number of received data frames was calculated. Results are presented in **Tab.** ***4***.

Tab. 4. Average number of received data frames.

	Distance [m]												
Power [dBm]	**0.5**	**1**	**2**	**5**	**10**	**20**	**30**	**40**	**50**	**60**	**70**	**80**	**90**
2	1000	1000	1000	1000	1000	1000	1000	643	0	905	0	0	0
4	1000	1000	1000	1000	1000	1000	1000	587	0	1000	1	188	0
6	1000	1000	1000	1000	1000	1000	1000	510	509	1000	428	996	0
8	1000	1000	1000	1000	1000	1000	1000	1000	521	1000	825	1000	10
10	1000	1000	1000	1000	1000	1000	1000	1000	505	1000	910	1000	39
12	1000	1000	1000	1000	1000	1000	1000	1000	898	1000	1000	1000	868
14	1000	1000	1000	1000	1000	1000	1000	1000	1000	1000	1000	1000	992
16	1000	1000	1000	1000	1000	1000	1000	1000	970	1000	1000	1000	997
18	1000	1000	1000	1000	1000	1000	1000	1000	999	1000	1000	1000	1000
20	1000	1000	1000	1000	1000	1000	1000	1000	1000	1000	1000	1000	1000

The data presented in Tab. 4 are also shown in Figure 1 to facilitate the analysis.

During the tests, the maximum distance was 90 m. This is due to the dimensions of the underground garage. This location was chosen over an open space because the aim was to test the system's performance under real-world operating conditions. For example, the telemetry system could be used to monitor various parameters within the underground parking facility, such as parking space availability, temperature, humidity, and the concentration of harmful gasses.

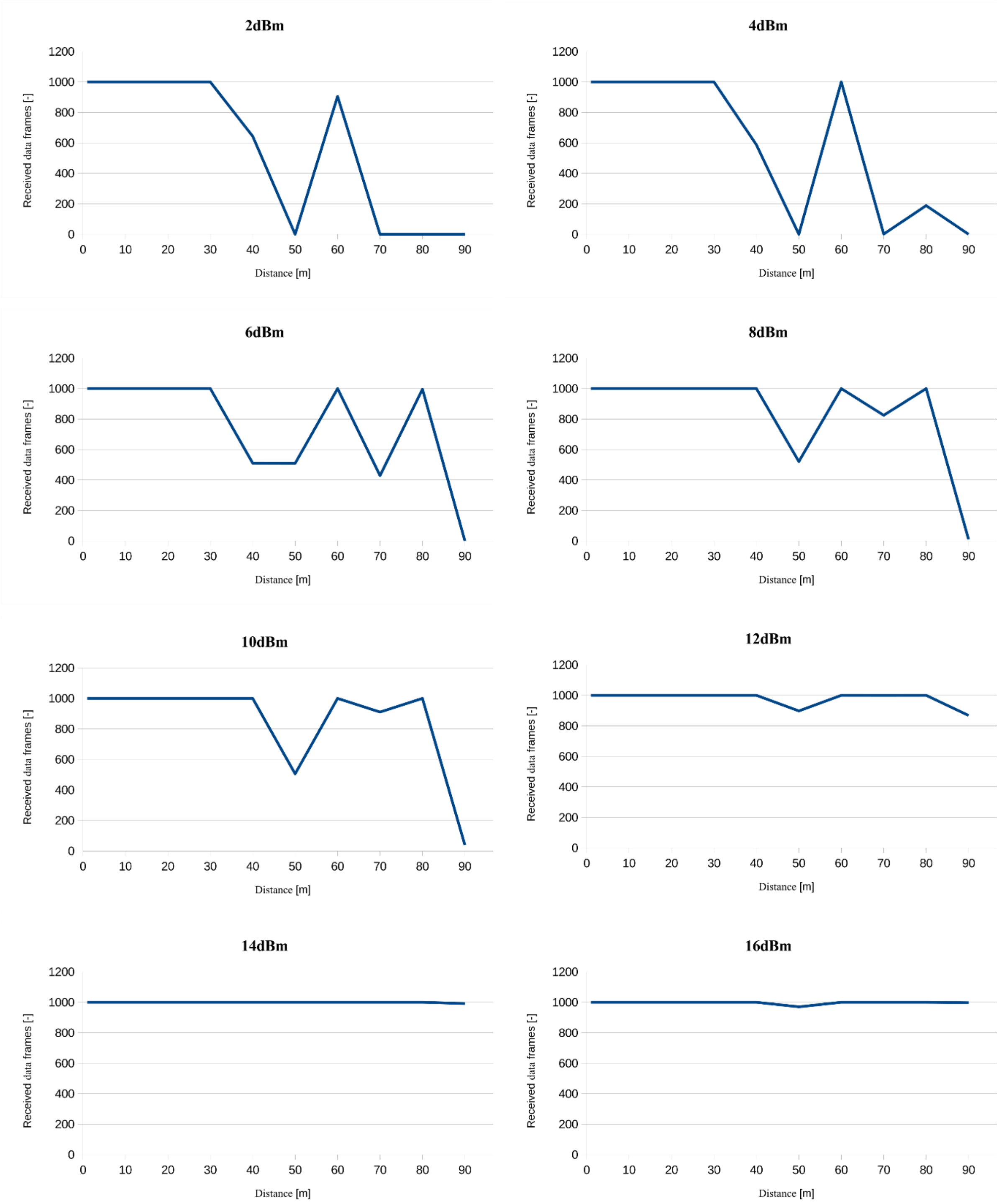
2dBm
4dBm
6dBm
8dBm
10dBm
12dBm
14dBm
16dBm
Received data frames [-]
Distance [m]
0
200
400
600
800
1000
1200
0 10 20 30 40 50 60 70 80 90

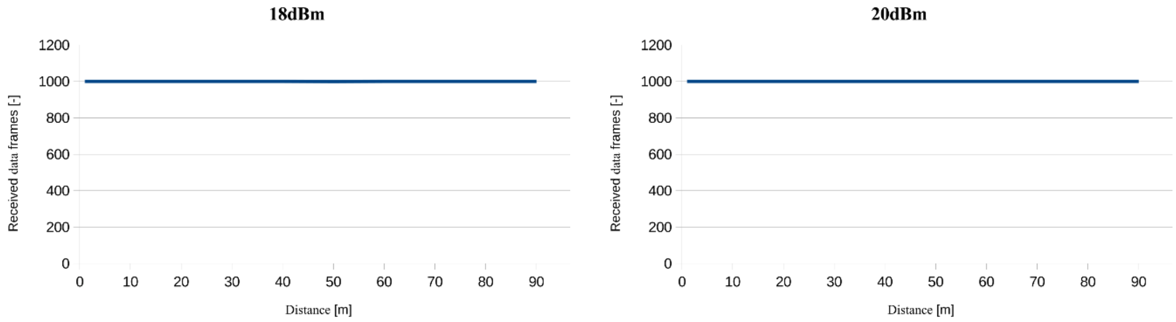

Figure 17. Average number of received data frames.

ESP-Now is a communication protocol developed by Esspressif. It reduces the OSI model (IEEE 802.11 physical layer specifications) to only one layer. Thanks to that, communication in faster and consumes less energy. During research the standard version on ESP-NOW was used. This version operates with Direct-Sequence Spread Spectrum (DSSS) with bitrate of 1Mbps. There is also another version (Long-Range Mode) designed for applications where long range is important. However, the data transfer speed is reduced to 512 Kbps or to 256Kbps.

Summary

During tests, the system worked correctly. The data sent by the sensor was received by the main unit and the main unit transmitted the confirmation of data reception. The ESP-NOW protocol was rapid. The transmission time of the data frame was less than 2 milliseconds. Moreover, one sensor cycle lasted about 143 milliseconds. However, the highest current consumption was during the sending process, but this process was very short. The time in which the encoder chip was used was as short as possible. The same situation was with the ESP32's WiFi module. All this proves that this sensor can operate on battery power. This makes it an ideal solution for wireless telemetry system.

It is still possible to reduce the current consumption of the sensor. There are many settings in ESP32 and encoder chips to configure. For example, it is possible to limit the maximum power of the sensor transmitting process or set a lower ESP32 CPU frequency. Moreover, it is also possible to set the lower value of maximum current of the LED on the encoder chip.

The encoder chip was equipped with multiple interfaces. It is also easy to configure. Moreover, the encoder can work with linear and rotary targets. These factors make it an ideal solution in many embedded systems.

If the encoder system is replaced with another compatible sensor, the system will also work properly. However, an appropriate correction of the data reading and data transmission frames will be necessary.

As expected, the operating range increased as the transmitter power increased. On the basis of the **Figure 17**, it can be clearly determined that the geometry of the room in which the system operates is of considerable importance. The data transmission problem is evident at distances of 50 meters and 70 meters. It likely stemmed from the metal ventilation ducts that run beneath the ceiling. Using sufficiently high transmitter power made it possible to eliminate this problem. When determining the number and placement of sensors, one should consider which approach is more advantageous: deploying a larger number of sensors closer together or using fewer sensors spaced further apart but equipped with larger batteries. In the future, it would also be worthwhile to investigate the data transmission range in other environments and using the ESP-NOW protocol mode designed for long distances.

Acknowledgment

The research was carried out as part of the project entitled *Direct drive steering gear for light and autonomous vehicles* (POIR.01.01.01-00-1177/21).

References

- Anderson, C. (2008), ‘The Petabyte age: because more isn’t just more–more is different’, Wired Magazine.
- Anggara Trisna Nugraha and Priyambodo, D., (2020), ‘Development of Rocket Telemetry in Chamber Gas Pressure Monitoring with the MPXV7002DP Gas Pressure Sensor’, Journal of Electronics, Electromedical Engineering, and Medical Informatics 2(3).
- Bhonde, P. and Panchwadkar, A., (2023), ‘Automatic detection of bearing faults’, Materials Today: Proceedings 77, pp. 586–591.
- Esspressif, (2026), ‘ESP32-C3 Datasheet. Version 2.4’.
- Esspressif, (2025), ‘ESP-IDF. Programming Guide’. [Online] [Retrieved June, 2003], https://docs.espressif.com/projects/esp-idf/en/v5.1/esp32/api-reference/network/esp_now.html
- Morollón, S., Urios, V. and López-López, P., (2022), ‘Home-Range Size and Space Use of Territorial Bonelli’s Eagles (Aquila fasciata) Tracked by High-Resolution GPS/GSM Telemetry’, Diversity 14(12).
- Niwa, H. and Sawai, Y., (2021). ‘Verification of the detection performance of drone radio telemetry for tracking the movement of frogs’, Drones 5(4).
- Nozomi Network (2025), ‘ESP-NOW. Protocol Analysis and Vulnerability Research’. [Online] [Retrieved June, 2026], https://cdn.prod.website-files.com/645a4534705010e2cb244f50/67e3ab1eec0b2be8f630f641_Nozomi-Networks-WP-ESP-NOW.pdf
- Saylan, Y. and Denizli, A., (2020), ‘Virus detection using nanosensors’, Nanosensors for Smart Cities.
- SKF, (2025), ‘Bearing damage and failure analysis’.
- Torkey, H., Ibrahim, E., Hemdan, E.E.D., El-Sayed, A. and Shouman, M.A., (2022), ‘Diabetes classification application with efficient missing and outliers data handling algorithms’, Complex and Intelligent Systems 8(1).
- Vasylenko, M.P. and Karpyuk, I.S., (2018), ‘Telemetry system of unmanned aerial vehicles’, Electronics and Control Systems 3(57).